Interaction parameters for blends containing polycarbonates: 2. Tetramethyl bisphenol A polycarbonate–styrene copolymers

C. K. Kim and D. R. Paul*
Department of Chemical Engineering and Center for Polymer Research, University of Texas at Austin, Austin, TX 78712, USA
(Received 6 June 1991; accepted 15 July 1991)

The phase behaviour of binary blends of tetramethyl bisphenol A polycarbonate (TMPC) and styrene copolymers with methyl methacrylate (SMMA) and acrylonitrile (SAN) has been re-examined as a function of copolymer composition. The interaction parameters for TMPC blends with each SAN copolymer and each SMMA copolymer were evaluated from the lower critical solution temperature (*LCST*) type phase boundary using the lattice fluid theory of Sanchez and Lacombe. From such information for several copolymer compositions, bare interaction parameters for various monomer unit pairs, ΔP^*_{ij}, were calculated using a binary interaction model. The interactions of styrene with the methyl methacrylate monomer units and with TMPC were weakly repulsive, while those of acrylonitrile with the styrene monomer units and with TMPC were strongly repulsive. The phase behaviour at the critical composition suggests that there exists an optimum content of MMA and AN in the copolymer at which the interactions are most favourable. Thermodynamic analysis based on the lattice fluid theory shows that the more favourable interactions of TMPC blends with some SAN and SMMA copolymers relative to polystyrene (PS) are achieved by different routes. A more negative energetic term caused by strong intramolecular repulsion between S and AN and a reduced compressibility effect are the main reasons why TMPC blends with certain SAN copolymers have higher *LCST* than do blends with PS. Compressibility or equation-of-state effects, especially the decrease in the characteristic temperature difference between TMPC and SMMA as MMA content increases, is the main reason why certain SMMA copolymers have higher *LCST* than PS when blended with TMPC. Note that the intramolecular repulsion between S and MMA is weak.

(Keywords: blends; tetramethyl polycarbonate; poly(styrene-*co*-methyl methacrylate); poly(styrene-*co*-acrylonitrile); lower critical solution temperature; equation of state)

INTRODUCTION

In the first paper of this series[1], a methodology for calculating the interaction parameter for a miscible blend system that exhibits a lower critical solution temperature (*LCST*) was described and applied to mixtures of tetramethyl bisphenol A polycarbonate (TMPC) and polystyrene (PS)[2–9]. This approach is based on the Sanchez–Lacombe lattice fluid theory, which accounts for the effects of compressibility or free volume. It requires accurate information about the equilibrium phase diagram of the blend, molecular weights of the components and the *PVT* properties of the components, so that their characteristic temperatures, pressures and volumes required by this equation-of-state approach can be evaluated. If the theory properly accounts for the effects of compressibility and all excess entropy issues stem from this cause, then the interaction parameter, ΔP^*, deduced should better represent the energetic interactions between the components than the Flory–Huggins interaction parameter, B (or χ). The latter theory is not consistent with *LCST* behaviour unless B is temperature-dependent and, hence, contains an excess entropy component. The quantity ΔP^* has been referred to by Sanchez[10–13] as the 'bare interaction energy' since effects of free volume have been stripped away such that it refers to the interaction in the close-packed dense state. Thus, there is reason to believe that ΔP^* is a more fundamentally useful quantity than B, especially for building a framework for correlating and predicting phase behaviour for copolymer systems using a matrix of interaction energies for monomer unit pairs. For copolymer systems, it permits the use of the phase-separation temperatures, in addition to copolymer composition limits for miscibility, in deducing the binary interaction parameters. This leads to the possibility of evaluating all monomer unit pair interaction parameters without recourse to other independent information. This is not possible by simply mapping regions of copolymer composition where miscibility exists, as others have pointed out[14–17]. Of course, all of this comes at the expense of a mathematically complex theory that requires the additional information about *PVT* behaviour of the components. In the current formulation, it is assumed that ΔP^* does not depend on temperature, i.e. the temperature dependence of the Flory–Huggins B (hence the *LCST*) stems entirely from equation-of-state effects, which limits the approach to systems without strong

* To whom correspondence should be addressed

0032-3861/92/102089-14

specific interaction. In principle, theories that overcome this limitation can be constructed[18].

The system TMPC–PS phase-separates on heating at temperatures that are relatively low, which limits melt processibility[1,7,9]. It has been shown previously[7,19–24] that addition of comonomer units to one of the homopolymers may be an effective way of raising the phase-separation temperature and solving the processibility problem. In fact, it has been suggested that modest amounts of either methyl methacrylate (MMA)[21] or acrylonitrile (AN)[7] added as a comonomer to the styrenic polymer will serve this function for blends with TMPC; however, too much of either comonomer leads to complete immiscibility with TMPC. The objective here is to extend the above-mentioned approach to copolymer systems and to deduce 'bare' binary interaction energies for the pairs S–MMA, TMPC–MMA, S–AN and TMPC–AN. The interaction for the TMPC–PS pair was established in the first paper of this series[1]. However, the phase diagrams for the TMPC–SMMA[21] and TMPC–SAN[7] blends established tentatively in earlier work contain some systematic errors and are not accurate enough for the current purpose. Thus, the experimental component of the present effort involved a more accurate determination of the phase diagrams and measurement of the necessary *PVT* characteristics of the component.

MATERIALS AND PROCEDURES

The materials used in this study are listed in *Table 1*. The tetramethyl bisphenol A polycarbonate (TMPC) is the same as that used previously[1,7,21]. The styrene–methyl methacrylate copolymers (SMMA) were synthesized by free-radical polymerization at 80°C using azobisisobutyronitrile as initiator except for two that were obtained commercially. The styrene-*co*-acrylonitrile copolymers (SAN) were obtained from several sources. The numerical value included as part of the code for these copolymers indicates the nominal per cent by weight of AN or MMA.

Blends of TMPC with copolymers were prepared by solution casting from tetrahydrofuran (THF) onto a hot glass plate. The cast solutions were dried at 60°C for 10 min until most of the solvent evaporated. The resulting films were further dried for a week in a vacuum oven at a temperature 20 to 30°C higher than the T_g.

Glass transition temperatures were measured by a Perkin–Elmer DSC-7 at a scanning rate of 20°C min^{-1}. The onset of the change in heat capacity was defined as the T_g. The cloud points caused by phase separation on heating, i.e. *LCST* behaviour, were measured both by the d.s.c. and light transmission methods described previously[1]. The reversibility of this phase-separation process by annealing at a lower temperature was also examined by d.s.c.[1].

The changes in specific volume of PMMA, SMMA copolymers and SAN copolymers as a function of temperature and pressure were measured using a density gradient column and a Gnomix *PVT* apparatus. Starting at 30°C, a sample was compressed along 31 isotherms, spaced about 15–20°C apart, up to about 270°C, with volume data recorded at pressure intervals of 10 MPa between 10 and 200 MPa along each isotherm. Samples were pressurized at a rate of about 20 MPa min^{-1}. The specific volume at zero pressure (or 1 atm) for each isotherm was obtained by extrapolation using the Tait equation.

BACKGROUND

The lattice fluid theory of Sanchez and Lacombe[10–14] will be used to illustrate the calculation of interaction parameters from phase behaviour. The equation of state has the form:

$$\tilde{\rho} + \tilde{P} + \tilde{T}[\ln(1-\tilde{\rho}) + (1 - 1/r)\tilde{\rho}] = 0 \quad (1)$$

where the reduced properties are defined as $\tilde{P} = P/P^*$, $\tilde{T} = T/T^*$, $\tilde{\rho} = \rho/\rho^*$ and r is the average number of occupied lattice sites per polymer chain. The characteristic properties are related to ε^* (monomer interaction energy), v^* (average mer hard core volume) and r (chain length) as follows:

$$\varepsilon^* = kT^* = P^*v^* \quad (2)$$

$$v^* = kT^*/P^* \quad (3)$$

$$r = \frac{M}{\rho^* v^*} = \frac{MP^*}{kT^*\rho^*} \quad (4)$$

where M is molecular weight. For a polymer liquid of large enough M, the equation of state reduces to a simple corresponding state equation ($1/r = 0$). The following simple reciprocal mixing rules are used for mixtures and for copolymers[12]:

$$1/v^* = \sum_i \phi_i/v_i^* \quad (5)$$

$$1/\rho^* = \sum_i w_i/\rho_i^* \quad (6)$$

$$1/r^* = \sum_i \phi_i/r_i \quad (7)$$

where w_i is the weight fraction and ϕ_i is the hard core volume fraction. The characteristic pressure of a mixture, P^*, is related to those of the pure components and the net interaction energy, ΔP^*, by:

$$P^* = \sum_i \phi_i P_i^* - \sum_{i<j}\sum \phi_i\phi_j \Delta P^* \quad (8)$$

For a binary blend of a copolymer composed of units 1 and 2 and a homopolymer composed of unit 3, the net interaction parameter between copolymer and homopolymer is assumed to be given by[25]:

$$\Delta P^* = \phi_1' \Delta P_{13}^* + \phi_2' \Delta P_{23}^* - \phi_1'\phi_2' \Delta P_{12}^* \quad (9)$$

where ϕ_1' and ϕ_2' are the close-packed volume fraction of units 1 and 2 in the copolymer.

RESULTS AND DISCUSSION

PVT *behaviour*

The *PVT* data were taken isothermally but are shown in *Figure 1* in the form of isobars at intervals of 30 MPa for selected polymers, all of which exhibit *PVT* behaviour typical of amorphous polymers[26–28]. At zero pressure, there is a simple slope change in $V(T)$ at the glass transition. The *PVT* behaviour in the glassy region to the left side of the line (a) reflects previous formation history. The 'dips' in the isobars for $P > 0$, in the temperature range between lines (a) and (b), are a consequence of the isothermal mode of operation. When measurements are taken along isotherms to the right of line (a), the increasing pressure eventually will force the equilibrium melt into a glassy state because increasing pressure results in a higher T_g. The glasses formed by

Table 1 Polymers used in this work

Abbreviation	Polymer	Copolymer[a] composition (wt%)	Density ($g\,cm^{-3}$)	Molecular weight[b]	Source
TMPC	Tetramethyl bisphenol A polycarbonate	–	1.083	$M_w = 33000$	Bayer AG
SAN 2	Poly(styrene-*co*-acrylonitrile)	2.7% AN	1.0487	$M_w = 204000$ $M_n = 93500$	Asahi Chemical
SAN 3.5		3.5% AN	—	$M_w = 211000$ $M_n = 96400$	Asahi Chemical
SAN 5.7		5.7% AN	1.0507	$M_w = 270000$	Asahi Chemical
SAN 6.3		–	–	$M_w = 343000$ $M_n = 92100$	Asahi Chemical
SAN 9.5		–	1.0568	–	Asahi Chemical
SAN 11.5		–	1.0587	–	Asahi Chemical
SAN 13.5		15.3% AN	1.0652	$M_w = 149000$ $M_n = 56300$	Asahi Chemical
SAN 14.7		14.7% AN	1.0640	$M_w = 182000$ $M_n = 83000$	Asahi Chemical
SAN 15.5		18.0% AN	1.0680	$M_w = 197000$	Asahi Chemical
SAN 19.7		19.7% AN	–	–	Asahi Chemical
SAN 25		25% AN	1.0775	$M_w = 152000$ $M_n = 77000$	Dow Chemical Tyril 1000
SAN 40		40% AN	1.0915	$M_w = 122000$ $M_n = 61000$	Asahi Chemical
SAN 70		69.7% AN	1.1291	–	Monsanto Co.
SMMA 5	Poly(styrene-*co*-methacrylate)	4.5% MMA	1.0626	$M_w = 281000$ $M_n = 98000$	Synthesized by Min[21]
SMMA 10		–	–	$M_w = 106000$ $M_n = 59100$	Synthesized
SMMA 15		–	–	$M_w = 106000$ $M_n = 60000$	Synthesized
SMMA 20		20.5% MMA	1.0746	$M_w = 268000$ $M_n = 110000$	Richardson Polymer Noan 81
SMMA 25		25.5% MMA	–	$M_w = 150000$ $M_n = 57000$	Synthesized by Min[21]
SMMA 30		–	–	$M_w = 109000$ $M_n = 60000$	Synthesized
SMMA 32		32.5% MMA	1.0795	$M_w = 167000$ $M_n = 78000$	Synthesized by Min[21]
SMMA 34		33.5% MMA	1.0938	$M_w = 217000$ $M_n = 871000$	Synthesized by Min[21]
SMMA 39		38.5% MMA	1.1031	–	Synthesized by Min[21]
SMMA 60		58.5% MMA	1.1317	–	Richardson Polymer RPC 100

[a]Determined by elemental analysis
[b]Molecular weight of SMMA and SAN copolymers were determined by g.p.c. using polystyrene standards

pressurizing the melt are generally more dense than those formed from the initial glass at the same temperature and pressure because of differences in their previous thermal history. Line (b) is defined as the intersection of the quasi-equilibrium PVT relation to the left of line (a) (non-equilibrium state) with the equilibrium melt PVT relation[28]. It is reasonable to interpret line (b) as denoting the pressure-dependent glass transition of the initial glassy state by analogy with the zero-pressure T_g. *Figure 2* shows the pressure dependence of the T_g of SAN 13.5 and PMMA determined by the intersection of the linear extrapolation from the initial glassy state and that from the equilibrium melt. Although there are several equations of state for representing PVT behaviour of polymer melts, the experimental data for both the melt and the glassy state can also be precisely fitted by the empirical Tait equation[26–29]:

$$V(P, T) = V(0, T)\{1 - 0.0894 \ln[1 + P/C(T)]\} \quad (10)$$

The parameter $C(T)$ is usually assigned an exponential temperature dependence:

$$C(T) = C_0 \exp(-b_1 T) \quad (11)$$

and $V(0, T)$, the specific volume at zero pressure, is well fitted by the polynomial:

$$V(0, T) = a_0 + a_1 T + a_2 T^2 \quad (12)$$

The coefficients in equations (11) and (12) for SAN

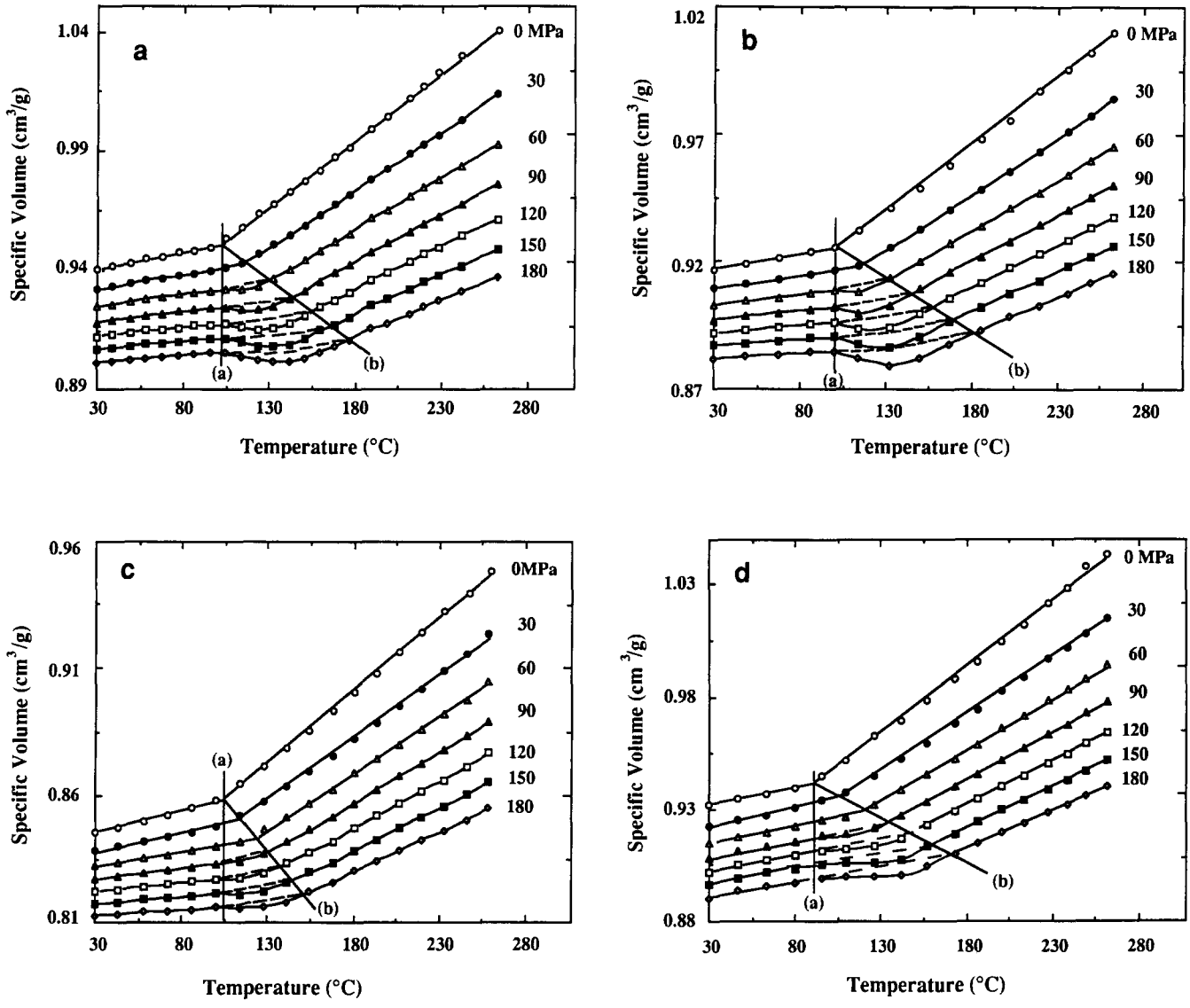

Figure 1 Specific volume of representative polymers as a function of temperature and pressure: (a) SAN 13.5, (b) SAN 40, (c) PMMA, (d) SMMA 20

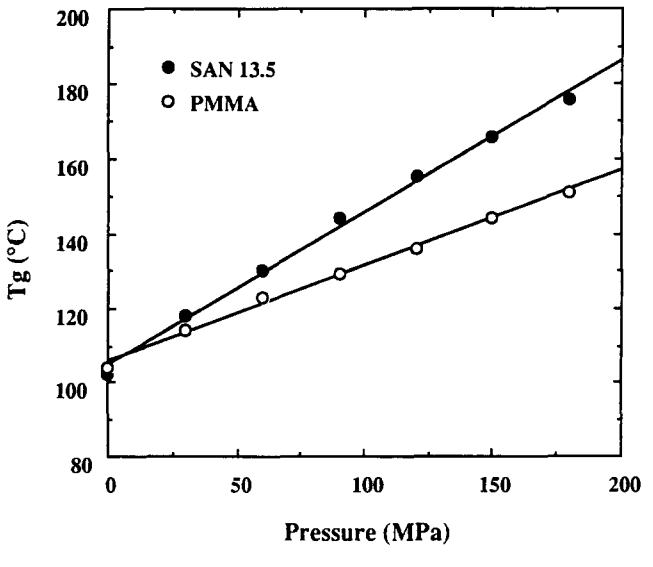

Figure 2 Pressure dependence of T_g for PMMA and SAN 13.5 obtained from *Figure 1*

copolymers, SMMA copolymers and PMMA are listed in *Table 2*.

Characteristic properties

Since equations of state can provide accurate fitting functions with which to analyse *PVT* data, they are a valuable tool in extrapolation of data beyond the range of actual experiments. It has been suggested that, even though the lattice fluid theory exhibits a systematic deviation from experiment at very high pressure, it still gives an accurate description of *PVT* behaviour in the moderate pressure range[11,30,31]. Non-linear least-squares methods of fitting experimental *PVT* data are widely used to obtain a set of characteristic parameters. Zoller[30] proposed a somewhat different fitting procedure using zero-pressure data and the Tait parameter. In this method, v^* and T^* are determined from the zero-pressure isobar while P^* is obtained from a comparison of the experimental and theoretical zero-pressure compressibility. *Tables 3* and *4* show characteristic parameters determined using these two different fitting methods over two different temperature ranges for SAN copolymers,

Table 2 Parameters for the Tait and zero-pressure volume equations for SAN copolymers, SMMA copolymers and PMMA

	SAN 2	SAN 13.5	SAN 15.5	SAN 40	SAN 70	PMMA	SMMA 20	SMMA 60
Glass state								
C_0 (bar)	3105	3312	3265	3657	3751	3767	2973	3550
b_1 (10^{-3} °C^{-1})	2.5043	2.6974	2.0115	2.9571	1.7436	4.7044	2.1480	4.3086
a_0 (cm^3 g^{-1})	0.9492	0.9352	0.9347	0.9122	0.8850	0.8421	0.9252	0.9795
a_1 (10^{-4} cm^3 g^{-1} °C^{-1})	1.5852	1.6594	0.7605	1.3603	0.5193	0.9223	1.6163	1.4142
a_2 (10^{-7} cm^3 g^{-1} °C^{-2})	1.2426	−1.9407	2.7390	−0.5160	3.3633	7.0113	1.0209	4.4158
Liquid state								
C_0 (bar)	2398	2384	2404	2893	3354	3000	2320	2610
b_1 (10^{-3} °C^{-1})	4.3763	3.9434	3.8578	4.4313	3.9230	5.0820	4.143	4.6112
a_0 (cm^3 g^{-1})	0.9233	0.9044	0.9016	0.8871	0.8528	0.8218	0.9063	0.8610
a_1 (10^{-4} cm^3 g^{-1} °C^{-1})	3.9355	4.2068	4.0365	3.4057	3.6159	2.8410	3.5702	3.3503
a_2 (10^{-7} cm^3 g^{-1} °C^{-2})	5.6848	4.0772	4.2061	4.9378	2.6336	8.1726	6.5323	6.9801

Table 3 Characteristic parameters for SAN copolymers, SMMA copolymers and PMMA obtained by non-linear least-squares fitting for the temperature ranges shown (pressure range = 0–50 MPa)

	Temperature range 150–200°C			Temperature range 220–270°C		
Polymer	ρ^* (g cm^{-3})	P^* (bar)	T^* (K)	ρ^* (g cm^{-3})	P^* (bar)	T^* (K)
PS	1.0191	3971	751	1.0922	3725	810
SAN 2	1.1099	3890	753	1.0935	3777	803
SAN 13.5	1.1297	4174	757	1.1089	3864	817
SAN 15.5	1.1334	4178	764	1.1125	3897	820
SAN 40	1.1519	4218	785	1.1311	4135	842
SAN 70	1.1883	4989	814	1.1688	4777	877
SMMA 20	1.1380	4155	743	1.1158	4001	797
SMMA 60	1.1960	4570	740	1.1910	4501	771
PAN[a]	1.2299	5357	853	1.2080	5192	909
PMMA	1.2601	5030	728	1.2564	5090	742

[a]Obtained by linear extrapolation of copolymer parameters to 100% acrylonitrile

Table 4 Characteristic parameters for SAN copolymers, SMMA copolymers and PMMA obtained from zero-pressure data and the Tait parameter for the temperature ranges shown

	Temperature range 150–200°C			Temperature range 220–270°C		
Polymer	ρ^* (g cm^{-3})	P^* (bar)	T^* (K)	ρ^* (g cm^{-3})	P^* (bar)	T^* (K)
PS	1.0998	4002	786	1.0836	3956	825
SAN 2	1.0990	4045	780	1.0880	3990	810
SAN 13.5	1.1168	4175	790	1.0998	4072	833
SAN 15.5	1.1206	4184	796	1.1048	4136	838
SAN 40	1.1416	4297	814	1.1298	4206	846
SAN 70	1.1777	4927	846	1.1601	4692	898
SMMA 20	1.1242	4121	775	1.1148	4240	797
SMMA 60	1.1871	4484	761	1.1784	4526	779
PAN[a]	1.2155	5249	873	1.1988	5977	927
PMMA	1.2512	4940	750	1.2460	5001	758

[a]Obtained by linear extrapolation of copolymer parameters to 100% acrylonitrile

SMMA copolymers and PMMA. Somewhat different values of the parameters were obtained if the temperature and pressure limits of these ranges were varied. Characteristic parameters determined by a non-linear least-squares method were used in subsequent interaction parameter calculations because those obtained by the latter method contain possible errors inherent in the extrapolation to zero pressure and the fitting procedure to obtain the Tait parameter. *Figure 3* shows how the characteristic parameters determined by the former method, in the temperature range 220–270°C, change as a function of AN weight or volume fraction in the SAN

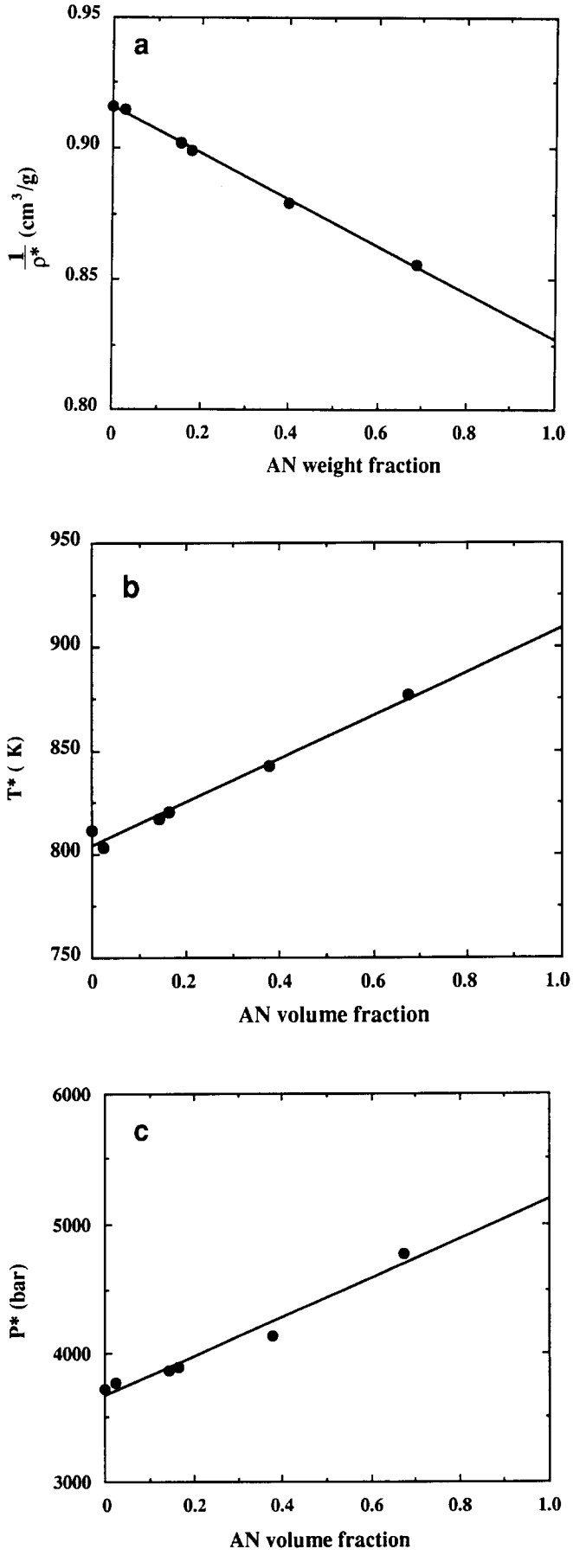

Figure 3 Characteristic parameters of SAN copolymers determined by non-linear regression method over the temperature range 220–270°C: (a) characteristic density; (b) characteristic temperature; (c) characteristic pressure

copolymers. Parameters for polyacrylonitrile (PAN) given in *Tables 3* and *4* were determined by linear extrapolation using equations (6) and (8). Note that the P_i^* terms are much larger than the ΔP_{ij}^* terms. As shown in *Figure 4*, comparing characteristic properties of SMMA 20 and SMMA 60 determined by experiment and those predicted by the mixing rules, the characteristic properties of SMMA copolymers follow the mixing rules well. Thus, characteristic properties for SMMA copolymers were determined by using those of the homopolymers and the mixing rules given in equations (5), (6) and (8).

Thermal behaviour

Figure 5 shows selected T_g behaviour for TMPC blends with SMMA copolymers containing 20% and 33% MMA; as expected from previous work[21], single, intermediate T_g values are observed for all compositions. TMPC blends with SMMA copolymers show phase separation on heating. However, it may be difficult to detect phase separation by optical observations because of the similarity of the refractive indices of TMPC and SMMA copolymers containing certain amounts of MMA (homopolymer refractive indices: $n_{TMPC} = 1.546$, $n_{PS} = 1.593$, $n_{PMMA} = 1.490$). To avoid this difficulty, phase-separation temperatures of blends were measured by the d.s.c. method described previously[1]. The d.s.c. scans in *Figure 6* show the glass transition behaviour of a blend after annealing for 5 min at a lower temperature (240°C, curve (a)) and a higher temperature (270°C, curve (b)) than the cloud point. The breadth of the glass transition region was determined as a function of annealing temperature, and the onset of a large change was taken as the phase-separation temperature[1]. The phase-separation curves for blends of the various SMMA copolymers with TMPC have a minimum (presumably the critical composition) at about the middle of the composition region as shown in *Figure 7*. As illustrated in *Figure 8*, the phase-separation temperature at 50% TMPC determined by the d.s.c. method is much lower than that obtained previously by optical means[21].

Figure 9 shows the T_g behaviour of TMPC blends with various SAN copolymers. For AN contents equal to or less than 18% by weight, a single intermediate T_g is observed at all blend proportions. On the other hand, blends of TMPC with SAN containing 19.7% AN or higher exhibited two glass transitions at all compositions. The miscibility boundary obtained here by THF hot casting is wider than that obtained earlier using methylene chloride as the casting solvent[7]. The observed phase behaviour can depend on the solvent used because of non-equilibrium phase separation induced by the well known $\Delta\chi$ effect[32–36] or when the two polymers become kinetically trapped into a homogeneous, but non-equilibrium, mixture below the glass transition[37]. To explore these aspects, phase reversibility was examined for TMPC blends with SAN 13.5 and SAN 15.5. *Figure 10* shows selected d.s.c. thermograms obtained at different annealing conditions for a blend containing 30 wt% SAN 15.5. This composition corresponds to the lowest phase-separation temperature among the blends having a single glass transition. Annealing above the phase-separation temperature (220°C) results in two glass transitions (curve (b)). After this treatment, the sample was quenched to 170°C, which is just below the cloud point, and annealed for 1 day. The d.s.c. thermogram obtained

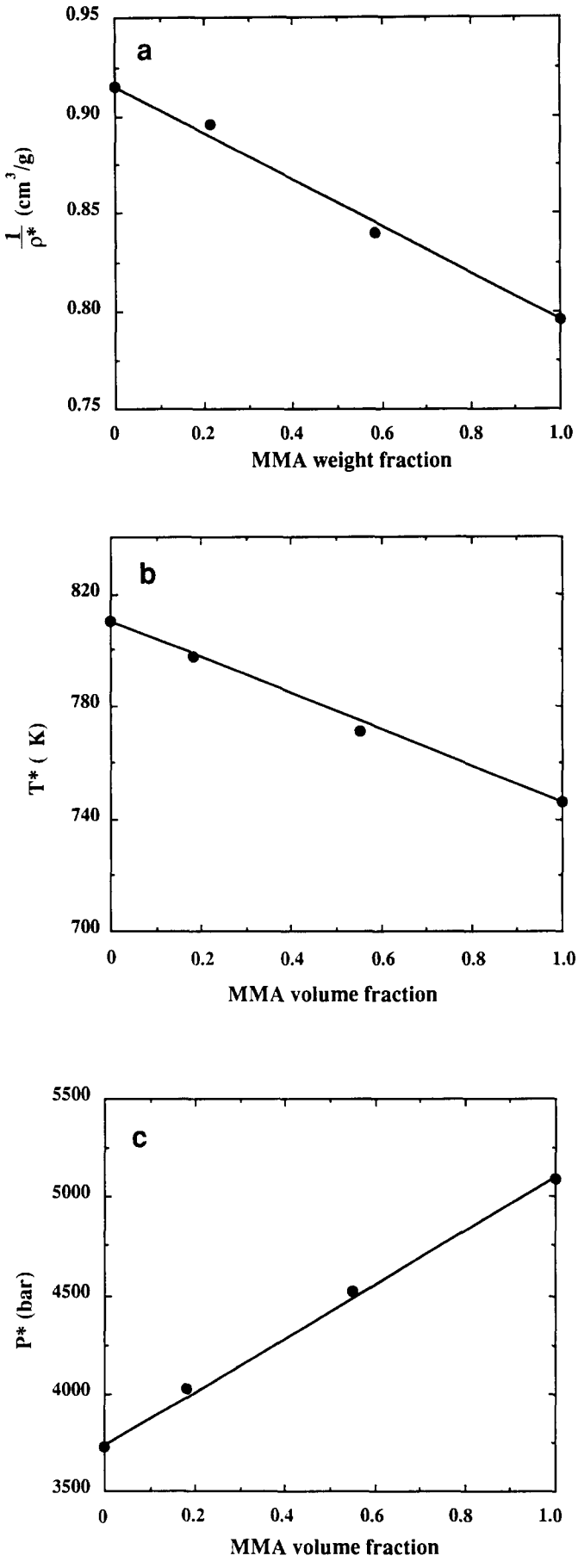

Figure 4 Comparison of characteristic properties of PS, PMMA, SMMA 20 and SMMA 60 obtained by experiment (●) and those predicted by mixing rules (——): (a) characteristic density; (b) characteristic temperature; (c) characteristic pressure

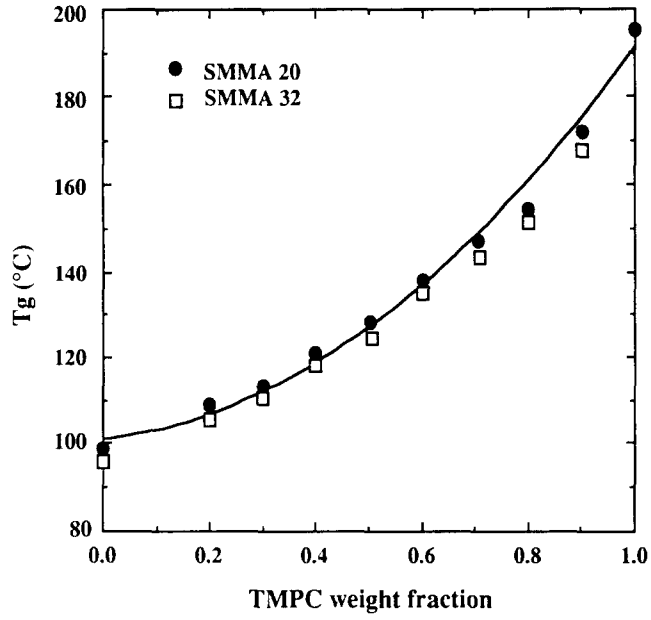

Figure 5 Selected T_g (defined by onset method) behaviour of TMPC blends with SMMA copolymers determined by d.s.c. at 20°C min^{-1}

after this (curve (c)) was the same as that in curve (a). These and other similar results suggest that the TMPC–SAN blends reported here as having a single glass transition are completely miscible at equilibrium and that the previously reported miscibility boundary reflects some error from a $\Delta\chi$ effect. The experimental phase-separation temperatures for four different TMPC–SAN systems are shown in *Figure 11*. TMPC blends with SAN copolymers containing between 3.5% and 11.5% AN did not phase-separate on heating. The critical composition appears to shift to the TMPC-rich direction as the AN content of the copolymer increases. On the other hand, for the TMPC–SMMA system, the MMA content did not affect the critical composition. A detailed discussion of the critical composition for both systems will be given in the next section.

Interaction parameters

To obtain the bare interaction parameter, ΔP^*, for any TMPC–copolymer pair, we employ two key assumptions discussed in the previous paper[1], viz. the measured phase boundary corresponds to the spinodal curve and ΔP^* does not depend on temperature. The first simplifies the calculation procedure while the second, if true, ensures that ΔP^* reflects only energetic issues and is free of further residual entropy effects. The latter assumption would begin to break down if strong specific interactions were involved. The calculation of ΔP^* for each TMPC–copolymer pair was carried out in the manner described previously[1], which amounts to forcing the equation for the spinodal condition derived from the Sanchez–Lacombe[12] theory to fit the measured phase-separation temperatures point by point for each composition. The characteristic parameters for TMPC were given previously[1] while those for the copolymers were computed from the data and equations mentioned above. *Figure 12* shows that the ΔP^* values so obtained for blends of TMPC with specific SMMA and SAN copolymers are essentially composition-independent. This is also true for the other SMMA and SAN copolymers not

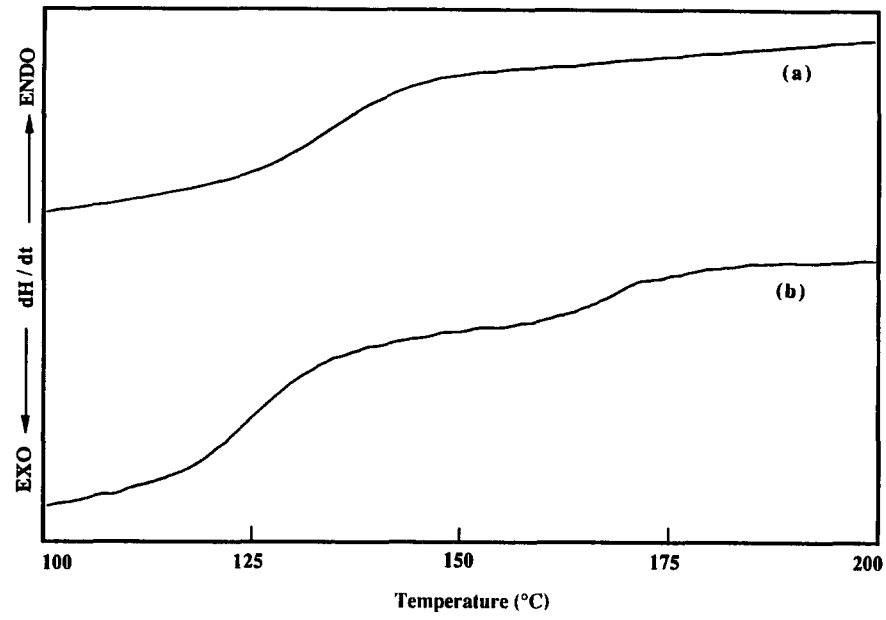

Figure 6 D.s.c. thermograms for a TMPC–SMMA 20 blend containing 50 wt% SMMA 20: (a) after annealing at 240°C for 5 min; (b) after annealing at 280°C for 5 min

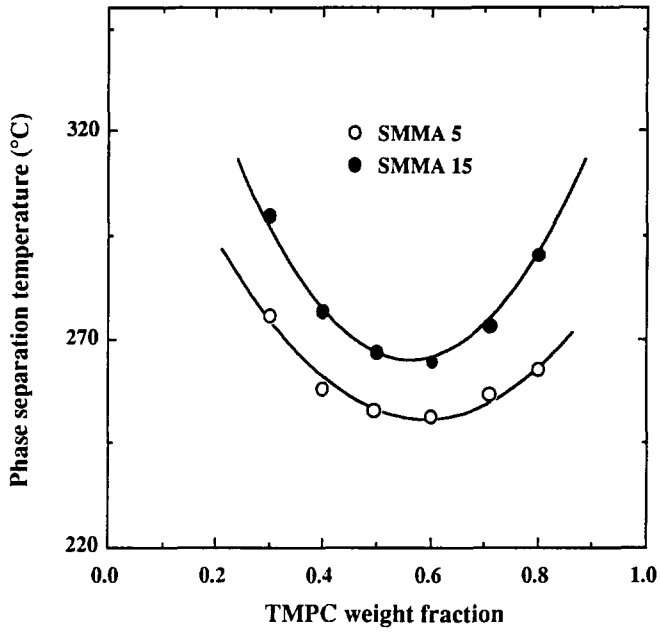

Figure 7 Phase-separation temperatures of TMPC blends with SMMA copolymers determined by d.s.c. method

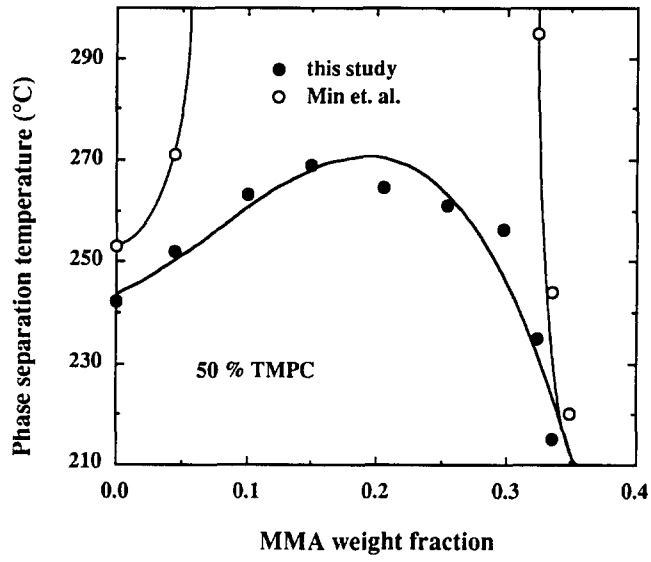

Figure 8 Comparison of phase-separation temperatures of TMPC blends with SMMA copolymers at 50% TMPC in blend

shown. *Figure 13a* shows that the minimum phase-separation temperature (this occurs near $\phi_{TMPC} \sim 0.5$) for a blend of TMPC with a given SMMA reaches a maximum when the MMA content of the copolymer is near 20% by weight. On the other hand, the computed ΔP^* for each copolymer–TMPC pair is negative and monotonically increases with MMA content of the copolymer (*Figure 13b*). Thus, there is no minimum in ΔP^* for the copolymer composition where the *LCST* is maximum. This would seem to contradict the general notion that systems with more favourable energetic interactions have higher *LCST*. Such behaviour is caused by the compressible nature or equation-of-state effects of these systems, as shown next.

For a binary mixture, the phase stability condition is given by[13,38]:

$$\frac{d^2G}{d\phi^2} = G_{\phi\phi} - \frac{(G_{\tilde{\rho}\phi})^2}{G_{\tilde{\rho}\tilde{\rho}}} > 0 \qquad (13)$$

where G is the Gibbs free energy per mer. In terms of the Sanchez–Lacombe theory[18,38], the indicated derivatives are given by:

$$G_{\phi\phi} = -2\tilde{\rho}\,\Delta\varepsilon^*_{12} + kT\left(\frac{1}{\phi_1 r_1} + \frac{1}{\phi_2 r_2}\right) \qquad (14)$$

$$G_{\tilde{\rho}\phi} = -[\varepsilon^*_{11} - \varepsilon^*_{22} - (1 - 2\phi_2)\,\Delta\varepsilon^*_{12}] + \frac{kT}{\tilde{\rho}}\left(\frac{1}{r_1} - \frac{1}{r_2}\right) \qquad (15)$$

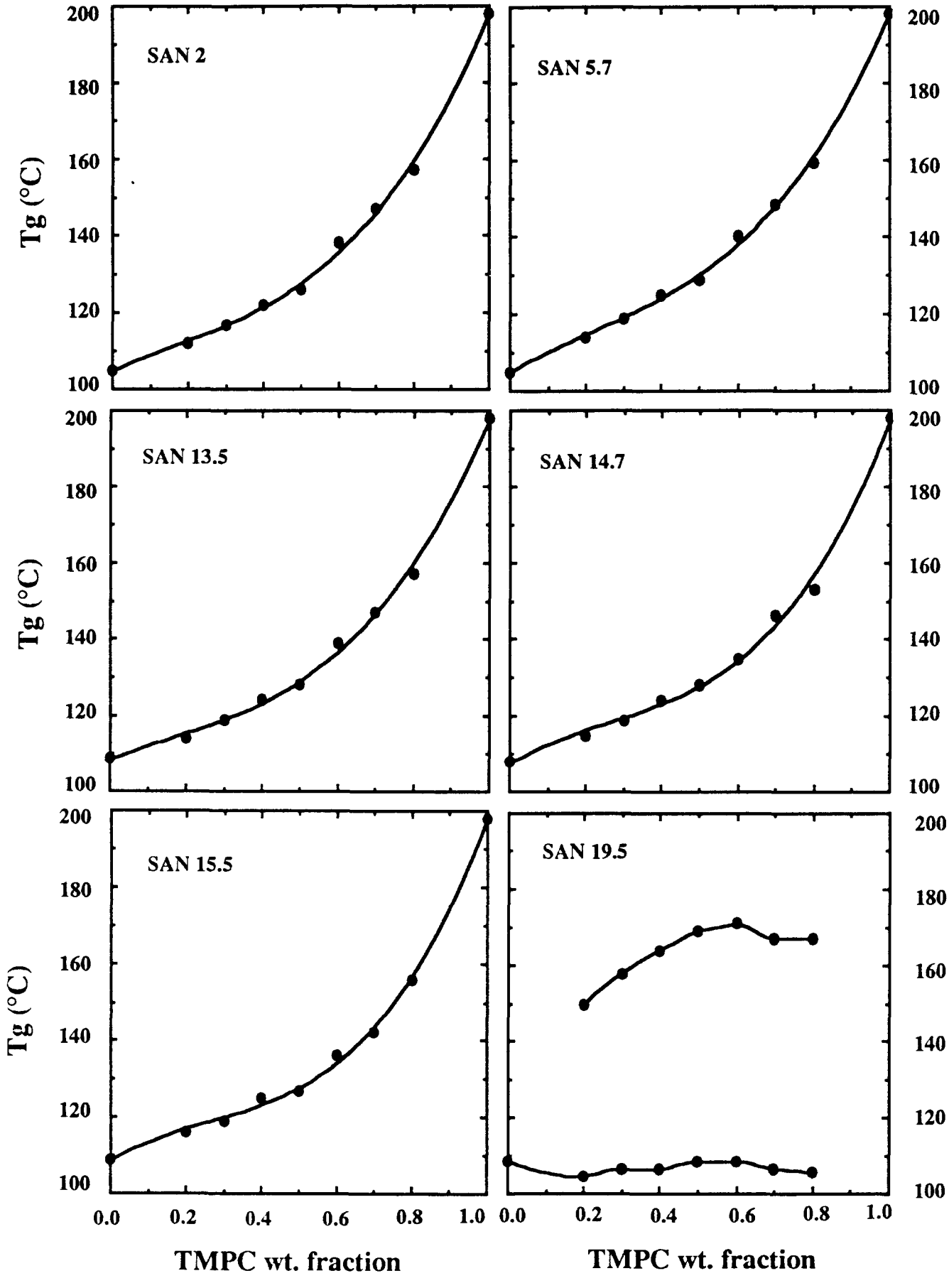

Figure 9 Selected T_g behaviour of TMPC–SAN blends determined by d.s.c. at 20°C min^{-1} (T_g by onset method)

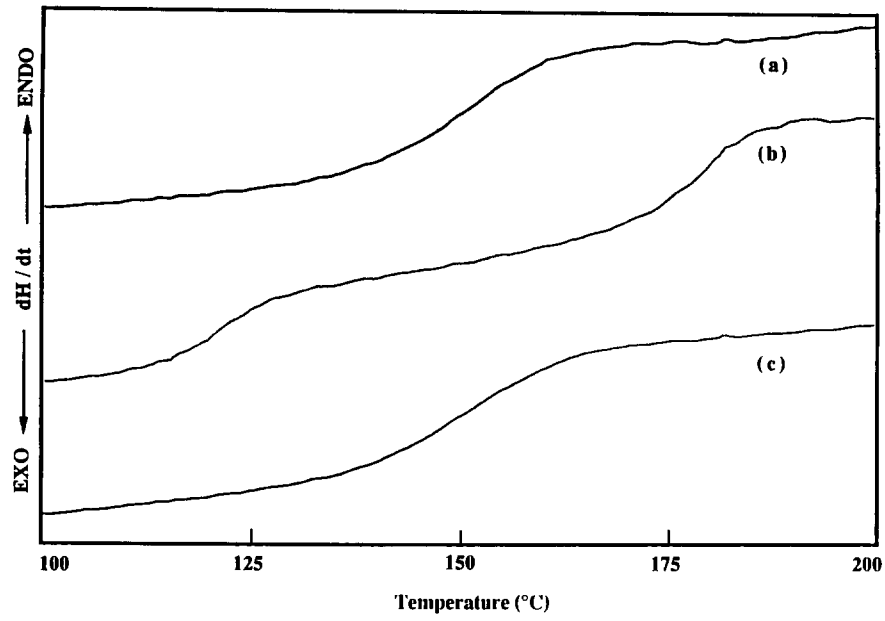

Figure 10 D.s.c. thermogram for TMPC–SAN 15.5 blend containing 70 wt% TMPC: (a) second scan after first scan to erase prior thermal history; (b) after annealing at 220°C for 5 min; (c) after annealing at 170°C for 1 day

$$G_{\tilde{\rho}\tilde{\rho}} = kT\left[\frac{2\ln(1-\tilde{\rho})}{\tilde{\rho}^3} + \frac{1}{\tilde{\rho}^2(1-\tilde{\rho})} + \frac{1}{\tilde{\rho}^2}\left(1-\frac{1}{r}\right)\right] \tag{16}$$

Note that the Sanchez–Lacombe theory based on lattice volume fractions[12,13] was used for calculation of interaction parameters. We have used the version based on lattice site fractions[10,11,18] in equations (14)–(16) and in the following qualitative discussion, since this permits a simple exposition of these arguments. This change of basis will not affect the outcome of the analysis. Since the combinatorial entropy terms are negligible at high molecular weight, $G_{\phi\phi}$ in equation (14) is given by:

$$G_{\phi\phi} \approx -2\tilde{\rho}\,\Delta\varepsilon_{12}^* \tag{17}$$

Since the ε_{ii}^*, or equivalently the characteristic temperatures T_i^*, are much larger than $\Delta\varepsilon_{12}^*$ and $1/r_i \sim 0$, equation (15) is approximately given by:

$$G_{\tilde{\rho}\phi} \approx -k(T_1^* - T_2^*) \tag{18}$$

The remaining derivative is related to the isothermal compressibility, and is given by[18]:

$$(G_{\tilde{\rho}\tilde{\rho}})^{-1} = \kappa\tilde{\rho}^3/v^* \tag{19}$$

where $\kappa \equiv -(\partial \ln v/\partial P)_T$ is the compressibility of the mixture. Finally, from equations (17), (18) and (19), the phase stability condition given by equation (13) reduces to:

$$\frac{d^2G}{d\phi^2} \approx -2\tilde{\rho}\,\Delta\varepsilon_{12}^* - \frac{1}{v^*}\left(\frac{T_1^* - T_2^*}{T}\right)^2 \kappa\tilde{\rho}^3 > 0 \tag{20}$$

The explanation for the observed phase behaviour of TMPC–SMMA blends is revealed in the two terms of equation (20) that comprise the stability condition. Here, we let the copolymer be component 1 and TMPC be component 2. Since the characteristic temperature for PS is larger than that for PMMA (see *Tables 3* and *4*), the characteristic temperature for an SMMA copolymer, T_1^*, becomes smaller as the MMA content increases. The reduced density of the SMMA copolymer, $\tilde{\rho}_1$, also becomes smaller as MMA content increases because $\tilde{\rho}_i < \tilde{\rho}_j$ when $T_i^* < T_j^*$ (ref. 18). If the energetics are favourable for mixing ($\Delta\varepsilon_{12}^* < 0$) and a *LCST* exists, then $\tilde{\rho}\,\Delta\varepsilon_{12}^*$ becomes less favourable as the MMA content increases since the reduced density of the mixture, $\tilde{\rho}$, decreases and $\Delta\varepsilon_{12}^*$ becomes less negative. At a given temperature, a smaller $\tilde{\rho}_i$ results in a larger isothermal compressibility of the copolymer. Therefore, the increased compressibility of the copolymer, relative to that of polystyrene caused by introducing MMA destabilizes the mixture and promotes phase separation. However, the characteristic temperature difference, $|T_1^* - T_2^*|$, becomes smaller as the MMA content of the copolymer increases (see *Tables 3* and *4*). The contribution of this term to phase stability becomes more favourable as the MMA content increases. In summary, energetic interactions ($\Delta\varepsilon_{12}^*$) and compressibility in equation (20) become less favourable for phase stability as the MMA content increases, while the characteristic temperature difference becomes more favourable. As the MMA content of the copolymer increases, there is competition among these terms. To see this more clearly, it is most convenient to equate the spinodal conditions from the Flory–Huggins theory and the lattice fluid theory to obtain the interaction energy, B_{sc}, needed by the former to satisfy the latter as described recently[1]. *Figure 14* shows the calculated B_{sc}, as a function of MMA content at 260 and 270°C. These values are all positive and become more positive as the temperature is raised (especially at low MMA contents). There is a minimum at around 20% MMA in the copolymer, which corresponds well to the maximum *LCST* shown in *Figure 13*. These results suggest that the observed increase in blend phase-separation temperature caused by adding small amounts of MMA to the styrenic polymer stems from equation-of-state effects, mainly a reduction in $(T_1^* - T_2^*)^2$, rather than from energetic effects, i.e. a more negative $\Delta\varepsilon^*$.

The ΔP_{ij}^* values for the binary pairs, TMPC–MMA and S–MMA, were determined by a linear least-squares

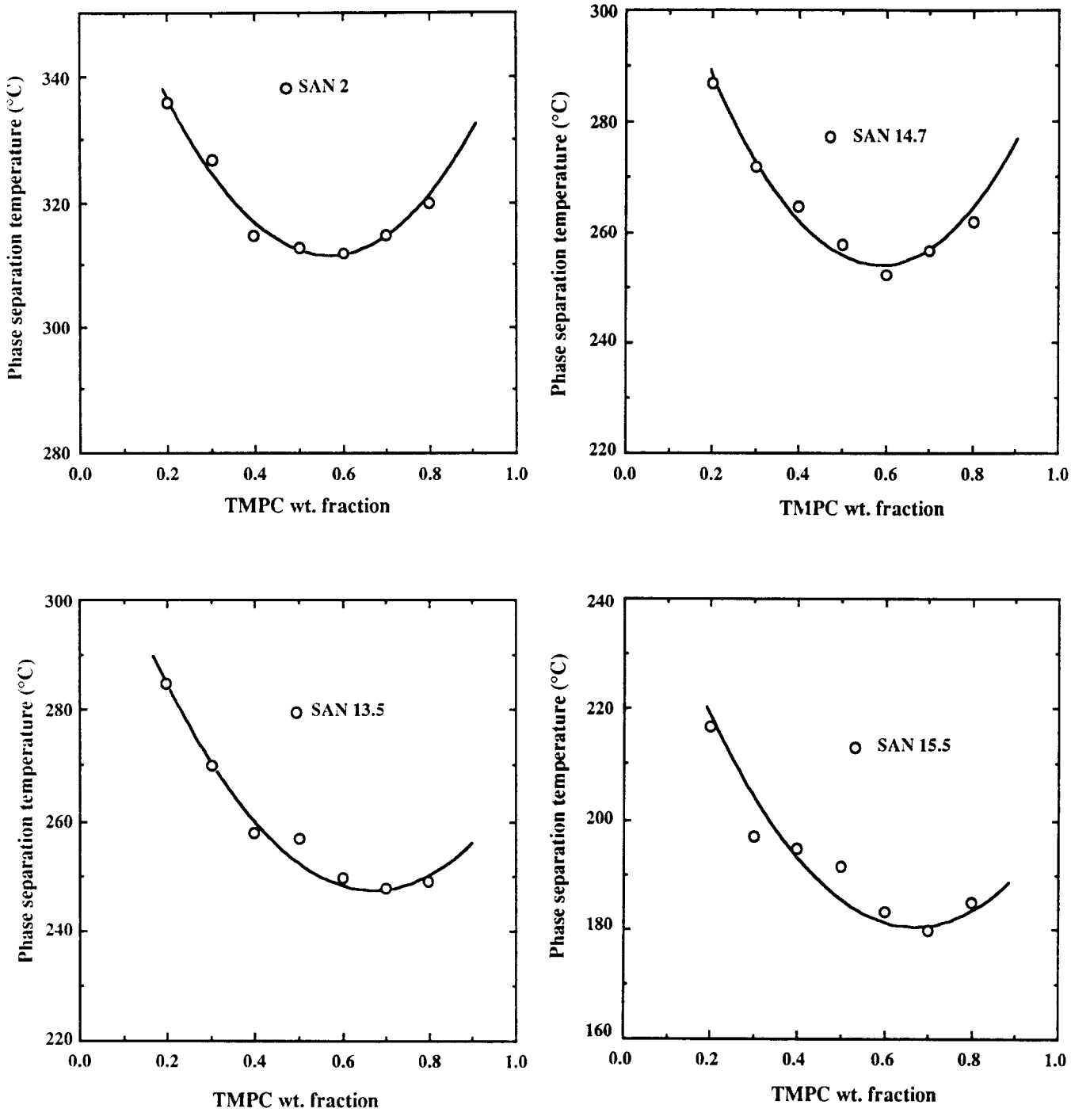

Figure 11 Phase-separation temperatures for TMPC blends with various SAN copolymers. Note that blends with SAN copolymers containing between 3.5 and 11.5% AN do not phase-separate prior to degradation (~330°C)

fitting of the values shown in *Figure 13* to equation (9). For this calculation, ΔP^*_{TMPC-S} was assigned the value (-0.17 cal cm^{-3}) determined previously. The remaining binary interaction energies were found to have positive values, $\Delta P^*_{TMPC-MMA} = 0.29$ cal cm^{-3} and $\Delta P^*_{S-MMA} = 0.15$ cal cm^{-3}, as expected. It is well known that blends of PMMA with TMPC and PS are immiscible.

Figure 15b shows ΔP^* calculated from the experimental phase-separation temperatures found for TMPC blends with SAN copolymers using the theoretical spinodal condition. Note that, since TMPC blends with SAN copolymers containing 5.7, 6.3, 9.5 and 11.5% AN do not show any phase separation prior to thermal decomposition or about 330°C, we cannot calculate ΔP^* for these blends. Values for $\Delta P^*_{TMPC-AN}$ and $\Delta P_{S-AN}{}^*$ were similarly calculated by a linear least-squares fitting of the ΔP^* in *Figure 15b* to equation (9). Relatively large positive values were obtained, i.e. 5.92 and 7.37 cal cm^{-3}, respectively. The net bare interaction energy for TMPC–SAN blends exhibits a minimum value at around 8.7% AN. *Figure 15a* shows the separation temperature for TMPC–SAN blends containing 50% of TMPC. The full circles are experimentally determined values. The full curve is the calculated result from the binary interaction energies mentioned above using the Sanchez–Lacombe spinodal condition for $\phi_{TMPC} = 0.5$ and $\bar{M}_w = 200\,000$. The predicted curve gives a good representation of the experimental data.

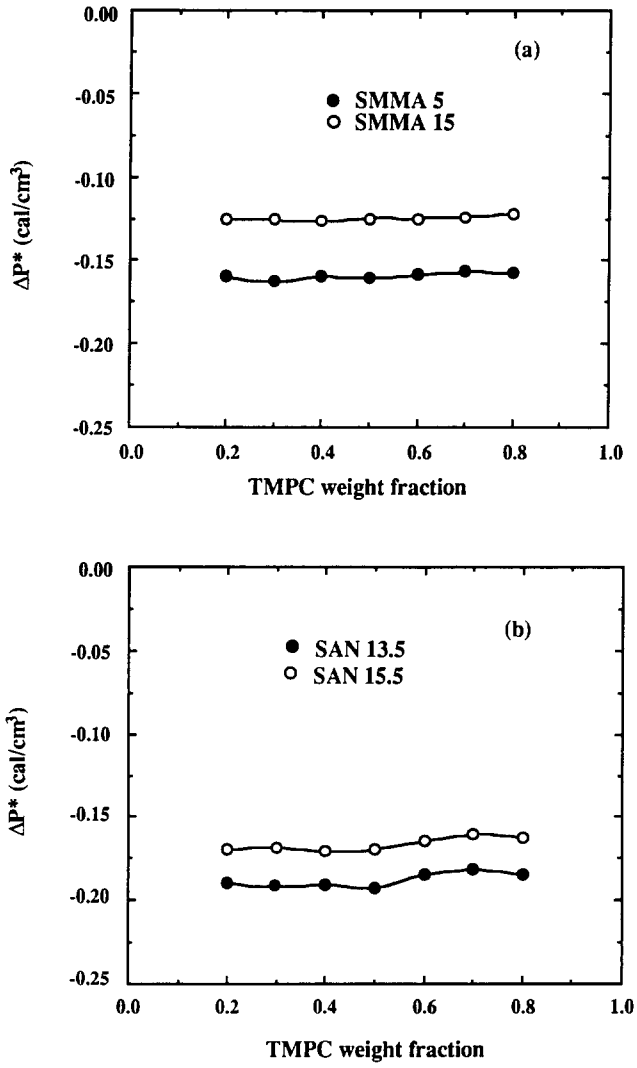

Figure 12 Bare interaction parameters for blends of TMPC with selected SMMA (a) and SAN (b) copolymers as a function of TMPC content of blend

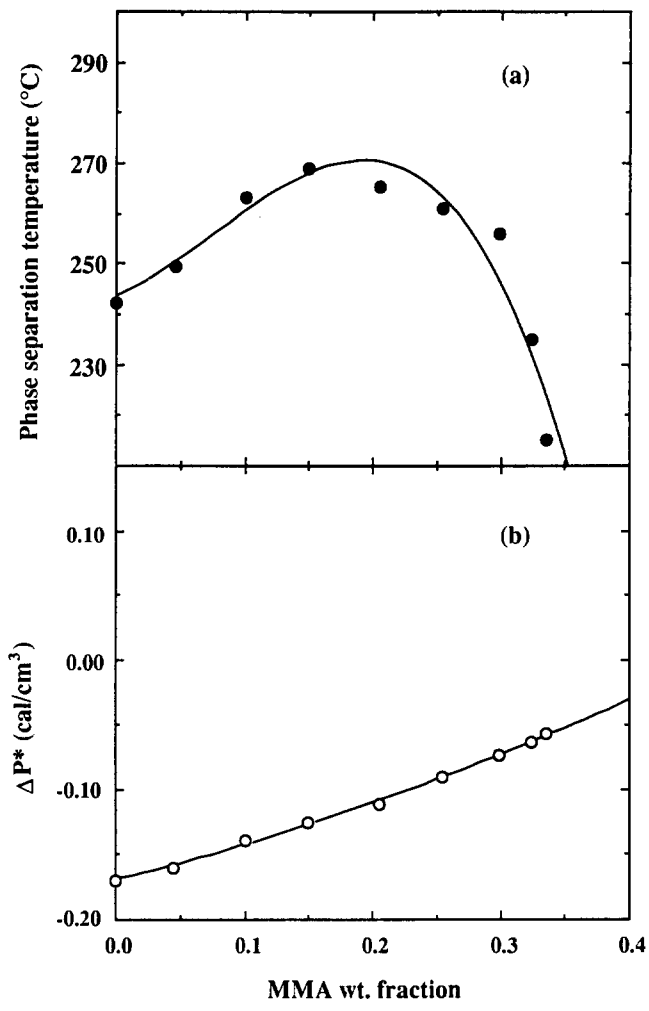

Figure 13 Effect of copolymer composition on the bare interaction parameter and phase-separation temperature for 50/50 TMPC–SMMA blends. The curve in (a) is the predicted phase-separation temperature using equation (9) for ΔP^* and assuming $\bar{M}_w = 200\,000$ for all SMMA copolymers, while the full circles are the experimentally determined phase-separation temperatures. The curve in (b) was calculated from equation (9), while the open circles are the ΔP^* determined from the experimental phase boundary and the lattice fluid theory

The major consequence of the above analysis is that the strong intramolecular repulsion between acrylonitrile and styrene units in the copolymer leads to more favourable energetic interactions between TMPC and certain SAN copolymers. This causes a dramatic increase in the *LCST*, which means that blends of TMPC with these copolymers, unlike polystyrene, are fully melt processible without concern for phase separation. Copolymers of higher AN levels are immiscible with TMPC owing to a dramatic decrease in the *LCST*.

The role of compressibility on phase stability is somewhat different when AN is copolymerized with styrene rather than MMA. In the following, we assign SAN as component 1 and TMPC as component 2. Since the characteristic temperature of PAN is larger than that of PS (see *Tables 3* and *4*), T_1^* and $\tilde{\rho}_1$ become larger as AN content increases. The smaller compressibility of SAN copolymers caused by $\tilde{\rho}_1$ increasing above that of polystyrene is favourable for phase stability. However, the $|T_1^* - T_2^*|$ term in equation (20) becomes larger as AN content increases. Thus, upon addition of small amounts of AN comonomer to the styrenic copolymer, the change in energetic interactions with TMPC and the compressibility increase the blend phase stability while the change in $(T_1^* - T_2^*)^2$ tends to decrease stability.

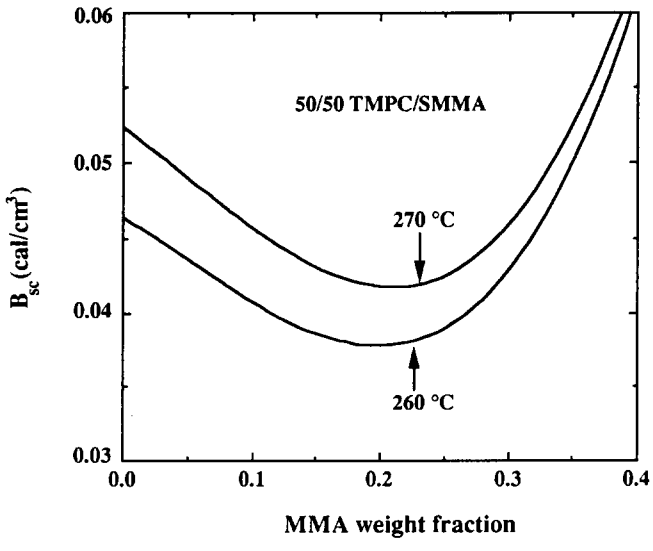

Figure 14 Flory–Huggins interaction parameters calculated from the spinodal condition, B_{sc}, at two different temperatures for TMPC–SMMA blends containing 50% TMPC as a function of copolymer composition

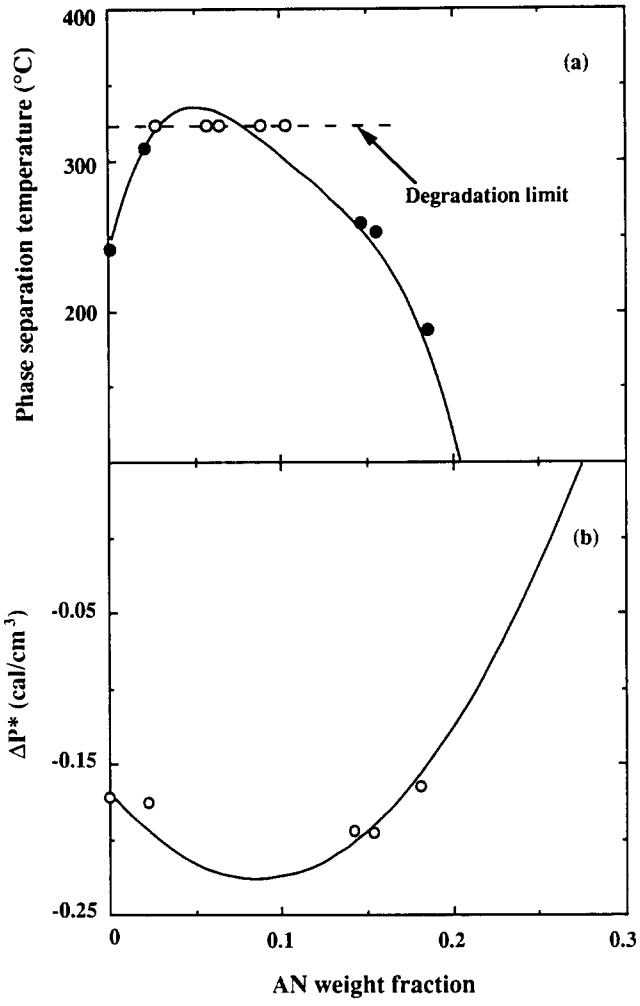

Figure 15 Effect of copolymer composition on the bare interaction parameter and phase-separation temperatures for 50/50 TMPC–SAN blends. The curve in (a) is the predicted phase-separation temperature using equation (9) for ΔP^* and assuming $\bar{M}_w = 200\,000$ for all SAN copolymers, while the full circles are the experimentally determined phase-separation temperatures (open circles indicate that decomposition occurs on heating, ~330°C, prior to phase separation). The curve in (b) was calculated from equation (9), while the open circles are the ΔP^* determined from the experimental phase boundary and the lattice fluid theory

Figure 16 shows that B_{sc} calculated at 260 and 270°C has a minimum around 6% AN.

The critical composition of TMPC blends with SAN copolymers (corresponding to the minimum phase-separation temperature), ϕ_c, shifts in the direction of the TMPC-rich side as the AN content of the copolymer increases. The molecular weights of the SMMA and SAN copolymers are several times larger than that of TMPC, as shown in *Table 1*. If molecular-weight effects dominated the value of ϕ_c, then blends of TMPC with PS, SMMA copolymers and SAN2 would have a TMPC-rich critical composition. However, these blends have ϕ_c near 0.5. The critical composition is relatively insensitive to the value of r when $r > 100$. Therefore, ϕ_c is dominated by equation-of-state terms, and the lattice fluid model predicts the critical point to be shifted towards the component with the smaller T_i^*. Since the characteristic

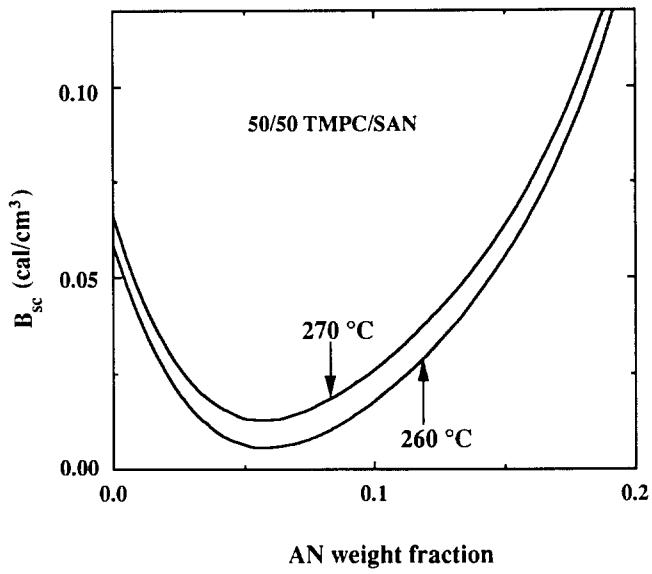

Figure 16 Flory–Huggins interaction parameter calculated from the spinodal condition, B_{sc}, at two different temperatures for TMPC–SAN blends containing 50% TMPC as a function of copolymer composition

Table 5 Interaction parameters (cal cm^{-3}) for various monomer pairs

	This paper		Other sources		
Interaction pair	ΔP_{ij}^*	B_{sc} at 30°C	ΔP_{ij}^*	B_{ij}	Method
S–MMA	0.13	0.19	0.13	–	PS/P(MMA–CHMA)[b] miscibility boundaries[39]
			–	0.181	Light scattering from PMMA/PS/solvent mixtures at 30°C[40–42]
			–	0.13	SANS analysis of PS–PMMA block copolymer at 30°C[43]
S–AN	7.37	7.25	–	4.99[a]	SAN/PMMA miscibility boundaries[15]
			–	8.0	SAN/SAN miscibility boundaries[44]
			–	6.9	Calorimetry of low-molecular-weight analogues at 25°C[45]
			–	8.14[a]	SAN/PMMA miscibility boundaries[46]
			–	6.8[a]	SAN/P(MMA–CHMA) miscibility boundaries[17]
			5.91	3.17	Calorimetry of low-molecular-weight analogues at 25°C[25]
TMPC–MMA	0.25	0.26	–	–	
TMPC–AN	5.92	6.01	–	–	

[a]Note that the interaction energy of S–MMA is from the work of Fukuda *et al.*[40–42]
[b]CHMA = cyclohexyl methacrylate

temperature of PAN is larger than that of PS, both the characteristic temperature of the copolymer and $\tilde{\rho}_1$ become larger as AN content increases. Thus, the differences between T_1^* and T_2^*, and between $\tilde{\rho}_1$ and $\tilde{\rho}_2$, increase as AN content increases. Sanchez and Balazs[18] have shown that stability is decreased for blends rich in the component having the lower T_i^* and $\tilde{\rho}_i$. Thus, the asymmetry of the pure component characteristic parameters causes the shift of the *LCST* to the TMPC-rich side as AN content of the copolymer increases. This asymmetry is small for SMMA blends with TMPC.

SUMMARY

Table 5 summarizes the binary interaction parameters computed here from the *LCST*-type phase boundary of TMPC blends with SMMA and SAN copolymers using the Sanchez–Lacombe lattice fluid theory. The S–AN and S–MMA interaction parameters obtained here correspond well to previously reported values. The miscibility region for TMPC blends with SAN copolymers reported here is somewhat broader than that obtained in the previous study[7], while the current region of miscibility is quite similar to that reported for SMMA copolymers[21]. However, the phase-separation temperatures reported here differ considerably in some cases, and the current values are more reliable.

Addition of either methyl methacrylate or acrylonitrile to the styrenic polymer initially increases the *LCST* but ultimately leads to immiscibility with TMPC. Based on thermodynamic analyses of these blends, the optimum comonomer content for the most favourable interaction with TMPC is around 6% of AN or 20% MMA. These optimum comonomer conditions, however, are achieved by different routes for SMMA and SAN copolymers. For TMPC blends with SMMA copolymers, the dominant cause for the optimum is compressibility or equation-of-state effects, while the weak intramolecular repulsion between S and MMA units is a minor factor. For TMPC blends with SAN copolymers, the strong intramolecular repulsion between S and AN units is the dominant cause for the optimum, while compressibility or equation-of-state effects are relatively less important.

ACKNOWLEDGEMENTS

This research was sponsored by the National Science Foundation Grant No. DMR-89-00704 administered by the Polymer Program. The authors wish to thank Professor I. C. Sanchez for his valuable assistance and advice.

REFERENCES

1 Kim, C. K. and Paul, D. R. *Polymer* 1992, **33**, 1630
2 Shaw, M. T. *J. Appl. Polym. Sci.* 1974, **18**, 449
3 Casper, R. and Morbizer, L. *Makromol. Chem.* 1977, **58/59**, 1
4 Humme, G., Rohr, H. and Serini, V. *Makromol. Chem.* 1977, **58/59**, 85
5 Yee, A. F. and Maxwell, M. A. *J. Macromol. Sci.–Phys.* 1980, **17**, 543
6 Wisniewsky, C., Marin, G. and Monge, P. *Eur. Polym. J.* 1984, **7**, 691
7 Fernandes, A. C., Barlow, J. W. and Paul, D. R. *Polymer* 1986, **27**, 1789
8 Yang, H. and O'Reilly, J. M. *Mater. Res. Soc. Symp. Proc.* 1987, **79**, 129
9 Guo, W. and Higgins, J. S. *Polymer* 1990, **31**, 699
10 Sanchez, I. C. and Lacombe, R. H. *J. Phys. Chem.* 1976, **80**, 2352
11 Sanchez, I. C. and Lacombe, R. H. *J. Polym. Sci., Polym. Lett. Edn.* 1977, **15**, 71
12 Sanchez, I. C. and Lacombe, R. H. *Macromolecules* 1978, **11**, 1145
13 Sanchez, I. C. 'Encyclopedia of Physical Science and Technology', Academic Press, New York, 1987, Vol. XI, p. 1
14 Kressler, J., Karasz, F. E. and Kammer, H. *Makromol. Chem.* 1990, **191**, 1623
15 Cowie, J. M. G. and Lath, D. *Makromol. Chem., Macromol. Symp.* 1988, **16**, 103
16 Cowie, J. M. G., Elexpuru, E. M. and McEwen, I. J. *J. Polym. Sci., Polym. Phys. Edn.* 1991, **29**, 407
17 Nishimoto, M., Keskkula, H. and Paul, D. R. *Macromolecules* 1990, **23**, 3633
18 Sanchez, I. C. and Balazs, A. C. *Macromolecules* 1989, **22**, 2325
19 Min, K. E. and Paul, D. R. *J. Polym. Sci., Polym. Phys. Edn.* 1988, **26**, 2257
20 Nishimoto, M., Keskkula, H. and Paul, D. R. *Polymer* 1991, **32**, 1274
21 Min, K. E. and Paul, D. R. *Macromolecules* 1987, **20**, 2828
22 Fowler, M. E., Barlow, J. W. and Paul, D. R. *Polymer* 1987, **28**, 1787
23 Stein, V. D. J., Jung, R. H., Iller, K. H. and Henders, H. *Angew. Makromol. Chem.* 1974, **36**, 89
24 Suess, M., Kressler, J. and Kammer, H. W. *Polymer* 1986, **27**, 957
25 Kim, J. H., Barlow, J. W. and Paul, D. R. *J. Polym. Sci., Polym. Phys. Edn.* 1989, **27**, 223
26 Quach, A. and Simha, R. *J. Appl. Phys.* 1971, **42**, 4592
27 Zoller, P. *J. Polym. Sci., Polym. Phys. Edn.* 1978, **16**, 1261
28 Zoller, P. *J. Polym. Sci., Polym. Phys. Edn.* 1982, **20**, 1453
29 Boyer, R. F. *Macromolecules* 1982, **15**, 774
30 Zoller, P. *J. Polym. Sci., Polym. Phys. Edn.* 1980, **18**, 157
31 Dee, G. T. and Walsh, D. J. *Macromolecules* 1988, **21**, 811
32 Bank, M., Leffingwell, J. and Thies, C. *Macromolecules* 1971, **43**, 1971
33 Robard, A. and Patterson, D. *Macromolecules* 1977, **10**, 706
34 Robard, A. and Patterson, D. *Macromolecules* 1977, **10**, 1021
35 Patterson, D. *Polym. Eng. Sci.* 1984, **22**, 64
36 Brannock, G. R. and Paul, D. R. *Macromolecules* 1990, **23**, 5240
37 Nishimoto, M., Keskkula, H. and Paul, D. R. *Polymer* 1991, **32**, 272
38 Sanchez, I. C. *Macromolecules* 1991, **24**, 908
39 Brannock, G. R. Ph. D. Dissertation, University of Texas at Austin, 1990
40 Fukuda, T. and Inagaki, H. *Pure Appl. Chem.* 1983, **55**, 1541
41 Fukuda, T., Nagata, M. and Inagaki, H. *Macromolecules* 1984, **17**, 548
42 Fukuda, T., Nagata, M. and Inagaki, H. *Macromolecules* 1986, **19**, 1411
43 Russell, T. P., Hjelm, R. P. and Seeger, P. A. *Macromolecules* 1990, **23**, 890
44 Schmitt, B. J., Kirste, R. G. and Jelenic, J. *Makromol. Chem.* 1980, **181**, 1655
45 Lai, C. H. Ph. D. Dissertation, University of Texas at Austin, 1988
46 Brannock, G. R., Barlow, J. W. and Paul, D. R. *J. Polym. Sci., Polym. Phys. Edn.* 1991, **29**, 413